Intestinal permeability, microbial translocation, changes in duodenal and fecal microbiota and their associations with alcoholic liver disease progression in humans

Luca Maccioni,[1] Bei Gao,[2] Sophie Leclercq,[3] Boris Pirlot,[1] Yves Horsmans,[4] Philippe de Timary,[5] Isabelle Leclercq,[1] Derrick Fouts,[6] Bernd Schnabl,[2,7] Peter Stärkel,[1,4]

[1]Institute of Experimental and Clinical Research, Laboratory of Hepato-gastroenterology, UCLouvain, Université Catholique de Louvain, Brussels Brussels, Belgium; [2]Department of Medicine, University of California San Diego, La Jolla, CA 92093, USA; [3]Institute of Neuroscience and Louvain Drug Research Institute, UCLouvain, Université Catholique de Louvain, Brussels, Belgium; [4]Department of Hepato-gastroenterology, Cliniques Universitaires Saint-Luc, Brussels, Belgium; [5]Department of Adult Psychiatry, Cliniques Universitaires Saint Luc, Brussels, Belgium; [6]J. Craig Venter Institute, Rockville, MD 20850, USA; [7]Department of Medicine, VA San Diego Healthcare System, San Diego, CA 92161, USA.

Supplementary material/data

Content:

Supplementary methods

Patients, methods

Inclusion-exclusion criteria

Additional inclusion criteria were first admission to the alcohol withdrawal unit and absence of previously diagnosed significant alcoholic liver disease.

Patients with diabetes were eligible for the study if they were on stable treatment (metformin, oral anti-diabetics with or without insulin) and a glycosylated hemoglobin level < 7% at admission.

Patients were excluded from the analysis if they had one of the following conditions:

- Inflammatory bowel disease or other chronic inflammatory or autoimmune diseases
- History of cancer within 5 years prior to admission
- Known liver disease of any other etiology
- Clinically significant cardio-vascular, pulmonary or renal co-morbidities
- Clinical and biochemical signs of active infection (t° > 37,5°C, viral syndrome, high CRP and high White Blood cell count)
- Administration of antibiotics, probiotics, glucocorticoids and nonsteroidal anti-inflammatory drugs during the two months preceding enrollment.

Fibroscan® measurements

Transient elastography measurements were performed using the Fibroscan® device (Echosens, Paris, France) by an experienced examiner blinded to the patient's data. Fibroscan® was considered as valid if at least 10 validated measurements were obtained with an interquartile range of less than 30%. The final result expressed in kPa was the median of all valid measurements obtained. We used the cut-offs for alcoholic patients proposed by Nguyen-Khac et al. (Aliment Pharmacol Ther. 2008; 28:1188-98), i.e. 7.8, 11, 19.5 kPa for F2, F3 and F4, respectively

Upper gastro-intestinal endoscopy and biopsy specimens

The standardized protocol of the alcohol withdrawal unit foresees a routine upper gastro-intestinal endoscopy within 72 hours of admission by an experienced endoscopist. Patients were slightly sedated with midazolam and 20mg of buthylhyosine was administered intravenously prior to the procedure in order to reduce intestinal peristaltic contractions. The endoscope was rapidly pushed under visual control into the distal duodenum. Care was taken to keep the transit time through the esophagus and the stomach as short as possible. Biopsies were taken from the distal duodenum with a single-use biopsy forceps (Boston Scientific, Galway, Ireland). During the first forceps passage, two duodenal biopsies were obtained for DNA extraction and 16S rRNA sequencing. Specimens were displayed on a sterile glass plate and rinsed repeatedly with sterile physiological solution to flush away non-adherent mucus and microbes, transferred into a sterile tube and immediately frozen in liquid nitrogen. Subsequent passages were performed to obtain additional biopsies which were preserved in RNA later (Invitrogen™, Thermo Fisher Scientific, Merelbeke, Belgium) or fixed in formalin.

Measurement of intestinal permeability

Intestinal permeability was assessed by measuring both the urinary excretion of the radioactive probe 51Cr-EDTA and the fecal albumin content by ELISA.

Briefly, after an overnight fast and emptying of the bladder, patients drank a Nutridrink (200 mL, 150 kcal/100 mL) (Nutricia) containing 50 µCi (1.85 MBq) 51Cr-EDTA. Two urine

collections were obtained: one from 0h to 4h representing the proximal intestine (duodenum, jejunum) and one from 4h to 24h representing the distal gut (ileum, colon). Radioactivity was measured in urine collections with a gamma counter (Cobra5003; Canberra Packard). Urinary excretion was expressed as the percentage of the ingested dose (ID) normalized to creatinine concentration (% ID/g creatinine). Permeability of the different parts was calculated from the respective urine collections. Total intestinal permeability was derived from the entire 24h urine collection.

In order to assess the fecal albumin content, proteins were extracted from at least 3 different parts of the stools of each patient using the extraction buffer provided in the kit (Human Albumin ELISA Kit, Immundiagnostik AG, Bensheim, Germany). Every single measurement was conducted in duplicate, and the data represent the mean of the different measurements performed.

Immunofluorescence

Intestinal samples were fixed in 10% formalin for 2 hours, washed and dehydrated in 30% sucrose for at least 4 hours and the included in OCT compound (Sakura, Kampenhout, Belgium). Five µm cryosections were rehydrated, blocked with phosphate buffer saline (PBS) 1x, 10% bovine serum albumin (BSA), and 3% milk. Sections were stained with the primary antibodies (Polyclonal rabbit IgG anti- ZO-1 (61-7300, Thermofisher, Merelbeke, Belgium) 1/100 and anti-human PLVAP (clone174/2, Abcam, Cambridge, United Kingdom) 1/50 overnight at 4 °C) followed by incubation with a secondary antibody conjugated with the fluorochrome Alexa Fluo 594 donkey anti-rabbit at 1/1000. Before imaging, nuclei were counterstained with 4', 6-diamidin-2-phenylindole (DAPI). Fluorescence multiplex immunostained slides were digitalized using a Pannoramic 250 FlashIII scanner (3DHistech, Budapest, Hungary).

PLVAP staining was quantified using the image analysis tool Author version 2017.2 (Visiopharm, Hørsholm, Denmark) and results were expressed as staining index (mean fluorescence intensity * stained area) on the duodenal biopsies.

Histology and morphometric indices

Since upper gastro-intestinal endoscopy is part of the standardized routine program of the alcohol withdrawal unit, biopsy specimens were routinely sent to the pathology department for examination by an experienced gastro-intestinal pathologist who generated a standard pathology report. After exclusion of any gastro-intestinal pathology susceptible to interfere with additional analyses of the specimens (e.g. celiac disease, Whipple's disease, collagenous sprue, inflammatory bowel disease, etc.), the duodenal sections were stained with Hematoxylin and Eosin and digitalized using a SCN400 slide scanner (Leica Biosystems, Wetzlar, Germany) at X20 magnification. Scanned slides were subjected to morphometric analysis with the image analysis tool Author version 2017.2 (Visiopharm, Hørsholm, Denmark). On each slide, villi were manually delineated and the major axis length of a simplified ellipse automatically drawn around the villus was measured. Results were expressed as the mean major axis length of at least 3 villi per slide.

Immunohistochemistry

Duodenal sections were stained overnight at 4°C with antibodies against CD45 (Mouse monoclonal anti-CD45 LCA, Clone 2B11+PD7/26) 1/30, CD68 (Mouse monoclonal anti-CD68, Clone PG-M1) 1/100, and CD3 (Mouse monoclonal anti-CD3, Clone L26) 1/200, and digitalized using a SCN400 slide scanner (Leica Biosystems, Wetzlar, Germany) at X20 magnification. Scanned slides were subjected to quantification analysis with the image analysis tool Author version 2017.2 (Visiopharm, Hørsholm, Denmark). On each slide, villi were first manually delineated and then automatically delineated along their perimeter. Stained pixels were detected at high resolution (x20) using a thresholding classification method. Thresholds were adjusted on representative stained vs not stained regions. The same

parameters were kept constant for all slides. Results were expressed as the mean stained area in percentage of at least 3 villi per slide normalized to the total surface area of the villi taken in consideration.

Reverse-Transcription and quantitative Real-Time Polymerase Chain Reaction

Primers were as follows: Villin: forward (F)-5'-CTGCTACATCATCCTGGCTATC-3' and reverse (R)-5'-GTCATCCATCTGTGTGGTGTAG-3';
IL1β; (F)-5'-GCACGATGCACCTGTACGAT-3'; (R)-5'-AGACATCACCAAGCTTTTTTGCT-3';
IFN-γ; (F)-5'-GCATCCAAAAGAGTGTGGAG-3'; (R)-5'-GCAGGCAGGACAACCATTAC-3';
IL17; (F)-5'-TTAGACCCCATCAAGGGTTAAAT-3'; (R)-5'-TGACCTTCTCTTCCCTCTCTCTT-3';
IL22; (F)-5'-AAAGCTGGTAGGAAAATGAGTCC-3'; (R)-5'-ACCTCTATCCTTTCCACCTTGAG-3';
Rpl-19: (F)-5'-CAAGCGGATTCTCATGGAACA-3'; (R)-5'-TGGTCAGCCAGGAGCTTC T-3'.

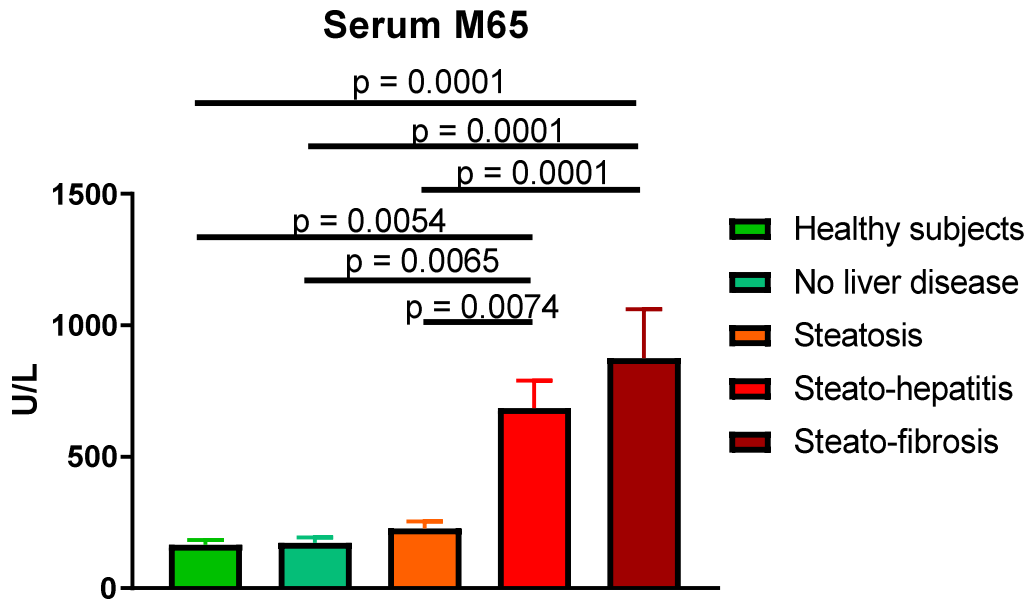

Supplementary Figure 1. Serum cytokeratin 18 (CK18-M65) according to different stages of liver disease.

Elevated CK18-M65 was only found in progressive ALD (steato-hepatitis and steato-fibrosis) independently from the development of fibrosis.

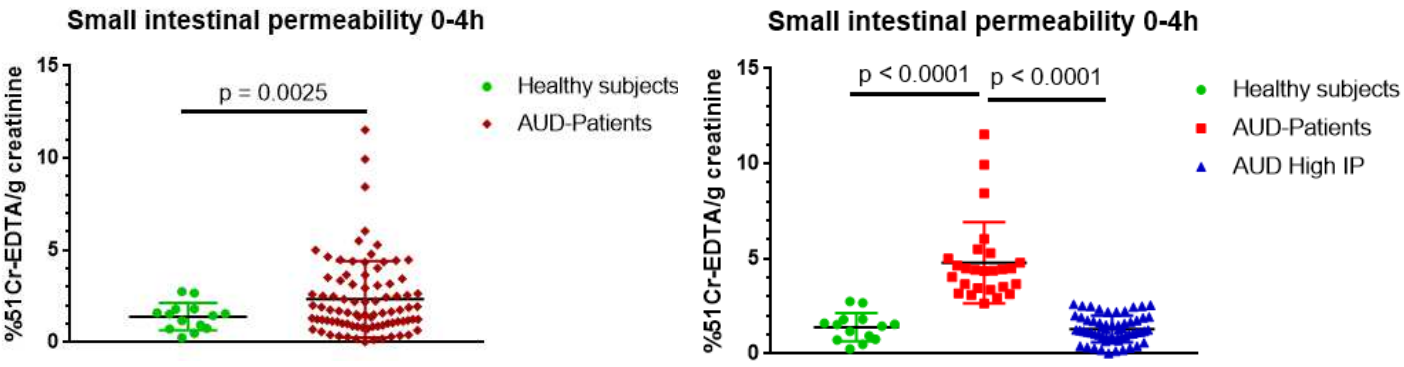

Supplementary Figure 2. Intestinal permeability (IP) in AUD patients in the small gut.

IP, based on ^{51}Cr-EDTA urinary excretion during the first four hours, representing the proximal small bowel fraction (duodenum, jejunum), increased significantly in AUD patients (n=86) compared to controls (n=14) (left). More detailed analysis revealed that only one-third of AUD patients showed significantly increased IP (n=34) compared to controls (right). This separation of subjects was calculated according to a deviance criterion at a threshold of 1.65 SDs of the mean of the control group.

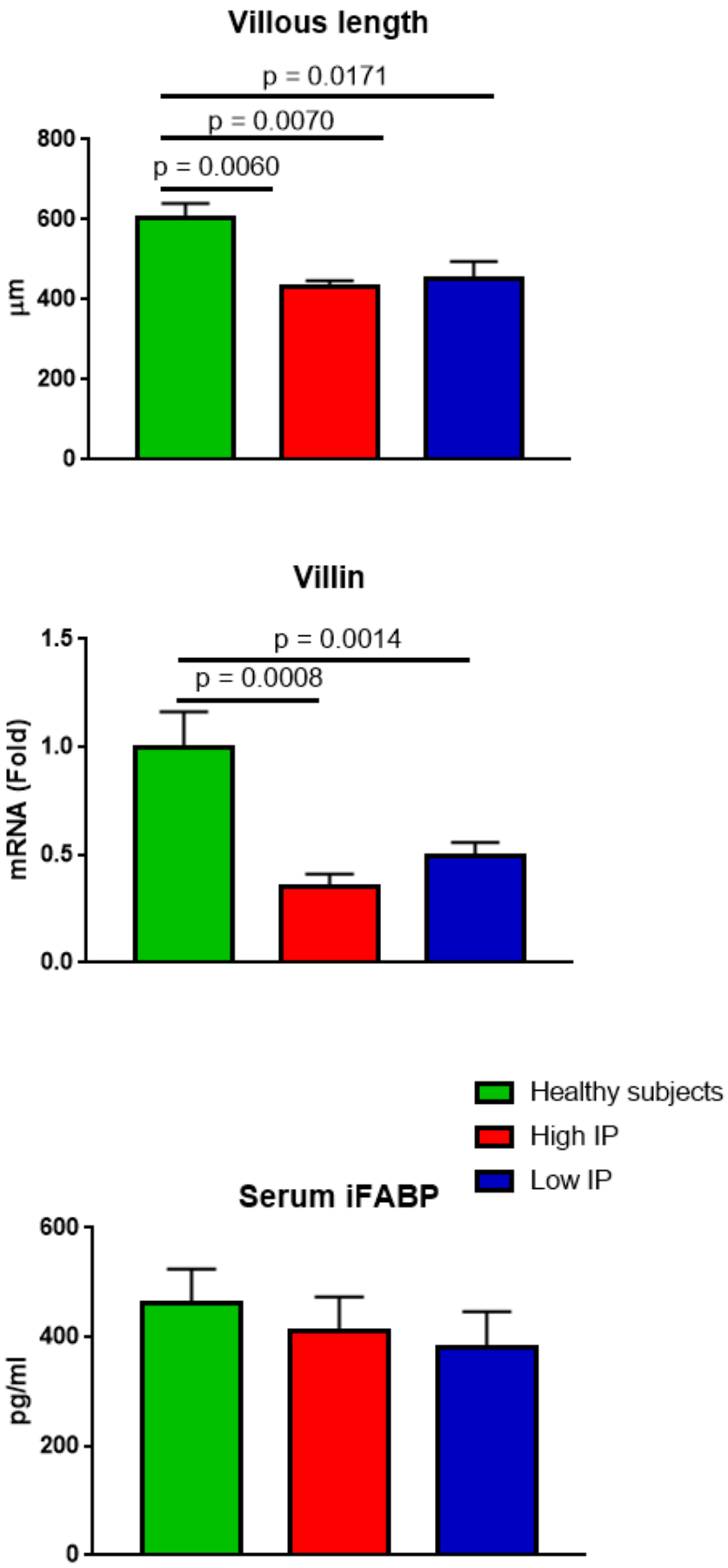

Supplementary Fig.3 Villi's length, Villin gene expression and enterocyte damage according to intestinal permeability (IP).

All the investigated parameters were similar when patients were split according to increased IP, measured by ^{51}Cr-EDTA urinary excretion.

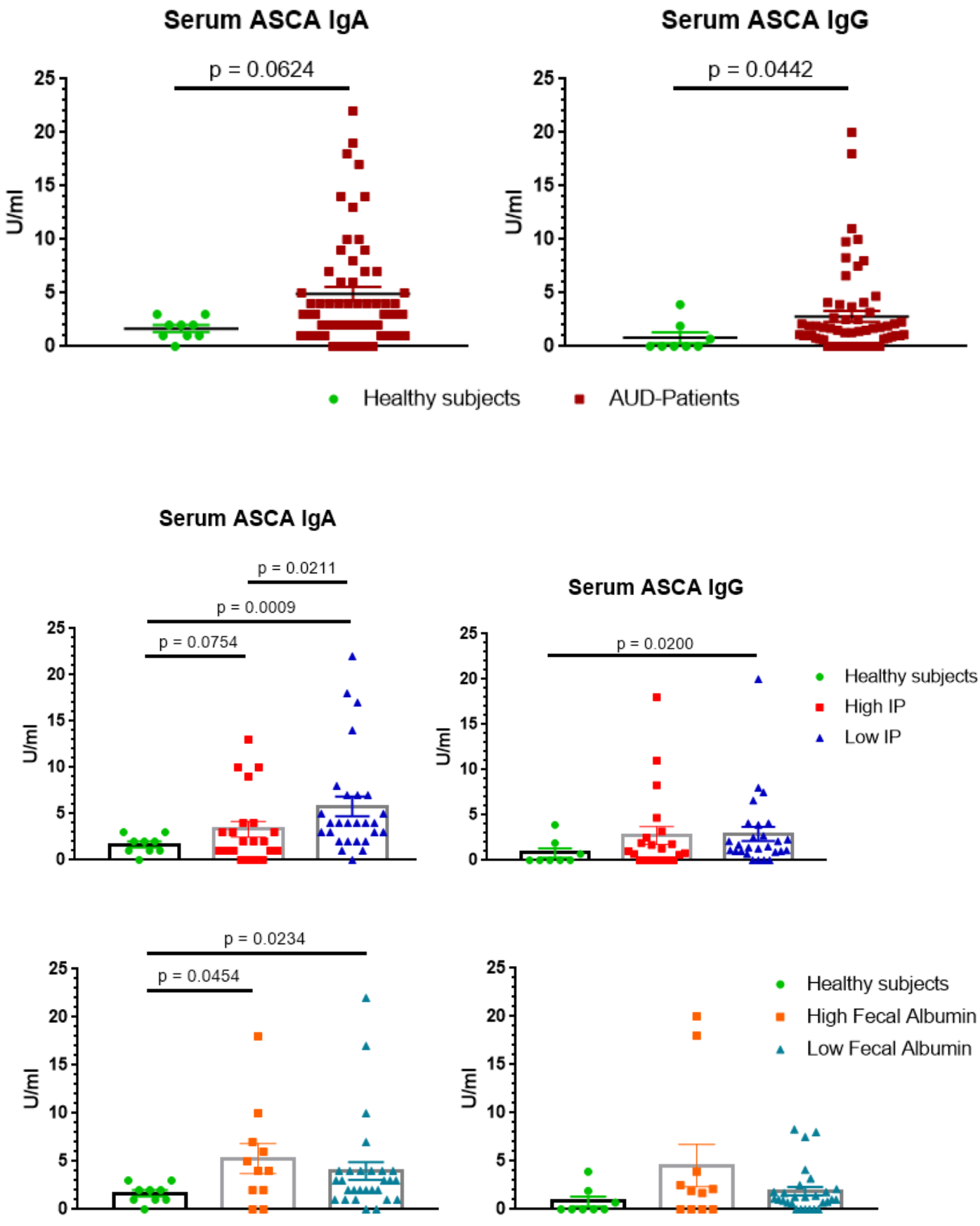

Supplementary Fig.4 Evaluation of serum ASCA levels in AUD patients in association with intestinal permeability (IP).

Serum ASCA levels increased significantly in AUD patients (n=60) compared to controls (n=9) (above) but independently of increased IP, measured by ^{51}Cr-EDTA urinary excretion (middle graphs) and fecal albumin content (lower graphs).

A

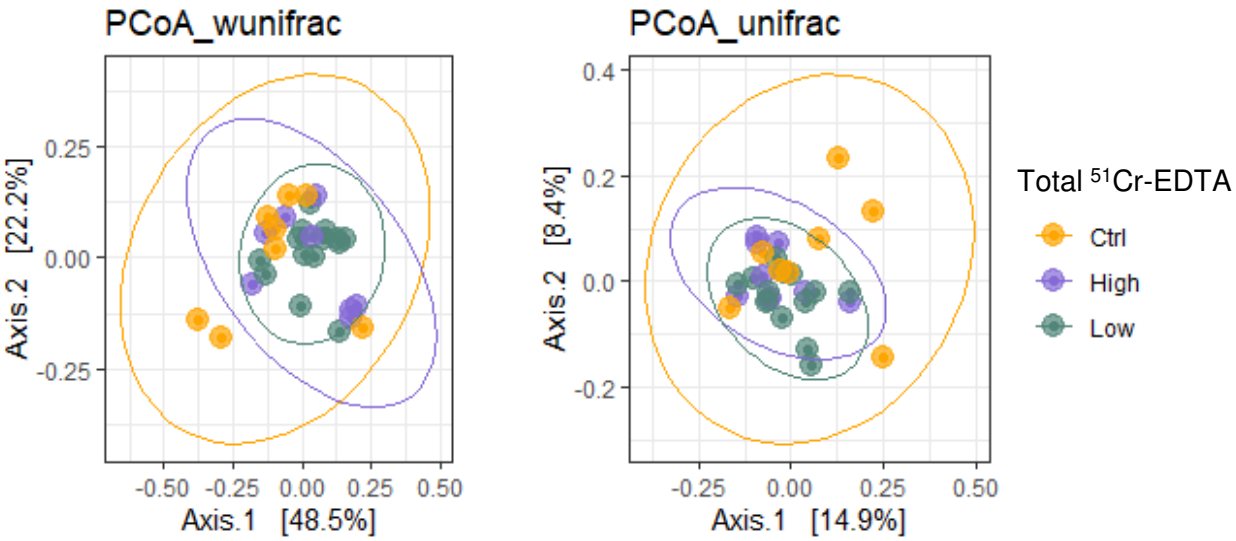
PCoA_wunifrac
Axis.2 [22.2%]
0.25
0.00
-0.25
-0.50 -0.25 0.00 0.25 0.50
Axis.1 [48.5%]
PCoA_unifrac
Axis.2 [8.4%]
0.4
0.2
0.0
-0.2
-0.25 0.00 0.25 0.50
Axis.1 [14.9%]
Total 51Cr-EDTA
Ctrl
High
Low

B

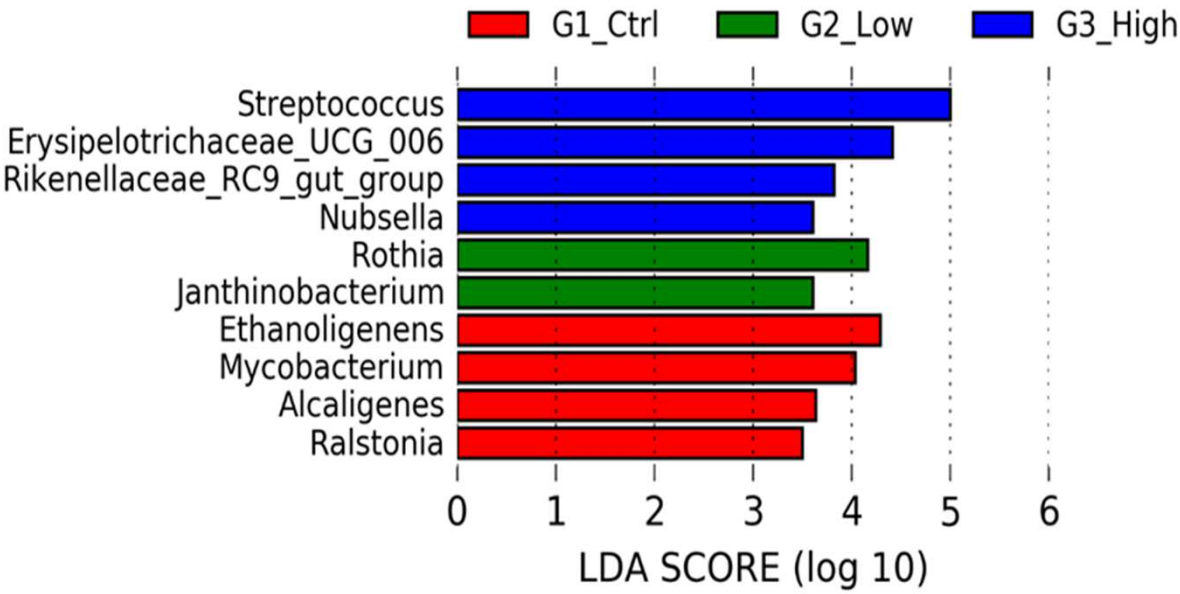
G1_Ctrl
G2_Low
G3_High
Streptococcus
Erysipelotrichaceae_UCG_006
Rikenellaceae_RC9_gut_group
Nubsella
Rothia
Janthinobacterium
Ethanoligenens
Mycobacterium
Alcaligenes
Ralstonia
0 1 2 3 4 5 6
LDA SCORE (log 10)

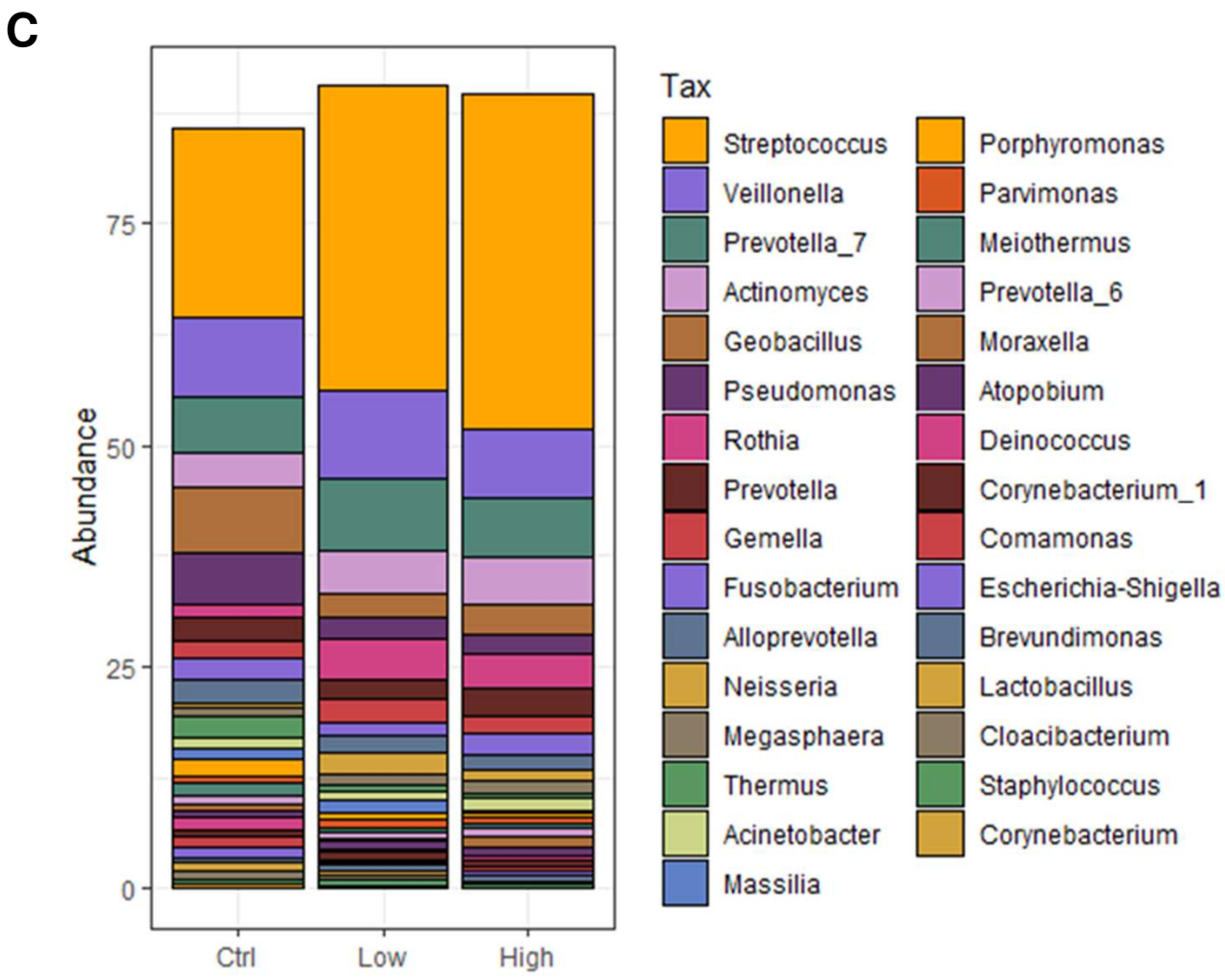

Supplementary Fig.5 Microflora composition of the duodenal mucosa-associated microbiota in association with intestinal permeability (IP).

(**A**) Microflora composition (β diversity) analysis of the duodenal microbiota showed no differences between AUD patients with high and low IP and healthy volunteers. (**B**) Results of linear discriminating analysis (LDA) effect size of AUD patients (high and low IP) compared to controls at the genus level. Different genera were overrepresented in the distal duodenum of AUD patients in relation to IP and healthy subjects (Ctrl).(**C**) Relative abundance of the different genera in the three groups. Only genera with detection in at least 2% are shown.

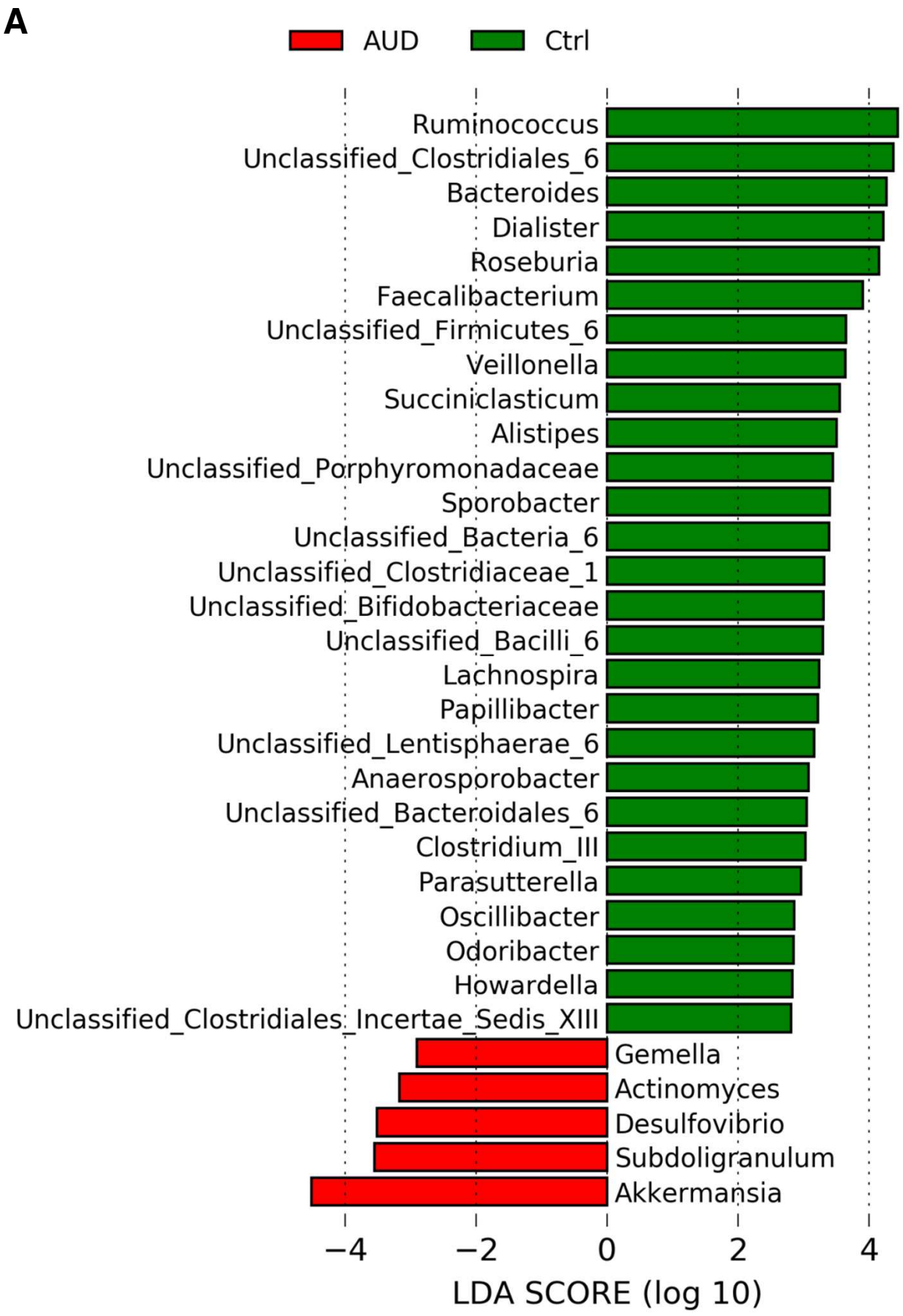
A
AUD
Ctrl
Ruminococcus
Unclassified_Clostridiales_6
Bacteroides
Dialister
Roseburia
Faecalibacterium
Unclassified_Firmicutes_6
Veillonella
Succiniclasticum
Alistipes
Unclassified_Porphyromonadaceae
Sporobacter
Unclassified_Bacteria_6
Unclassified_Clostridiaceae_1
Unclassified_Bifidobacteriaceae
Unclassified_Bacilli_6
Lachnospira
Papillibacter
Unclassified_Lentisphaerae_6
Anaerosporobacter
Unclassified_Bacteroidales_6
Clostridium_III
Parasutterella
Oscillibacter
Odoribacter
Howardella
Unclassified_Clostridiales_Incertae_Sedis_XIII
Gemella
Actinomyces
Desulfovibrio
Subdoligranulum
Akkermansia
−4
−2
0
2
4
LDA SCORE (log 10)

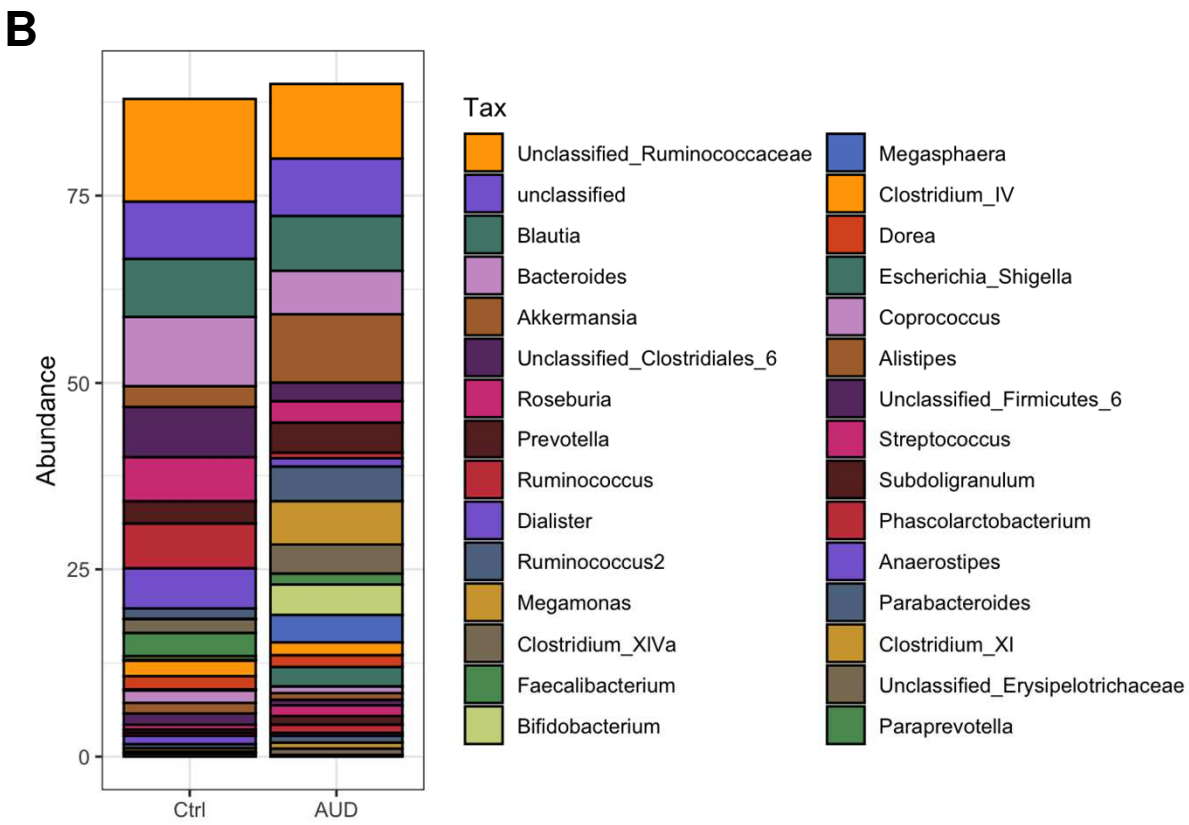

Supplementary Fig.6 Linear discriminating analysis (LDA) and relative abundance of bacterial genera in the stool of AUD patients and healthy volunteers.

(**A**) Higher abundance of *Gemella*, *Actinomyces*, *Desulfovibrio*, *Subdoligranulum* and *Akkermansia* characterized the stools of AUD patients compared to controls. (**B**) Relative abundance of the different genera in the two groups. Only genera with detection in at least 2% are shown.

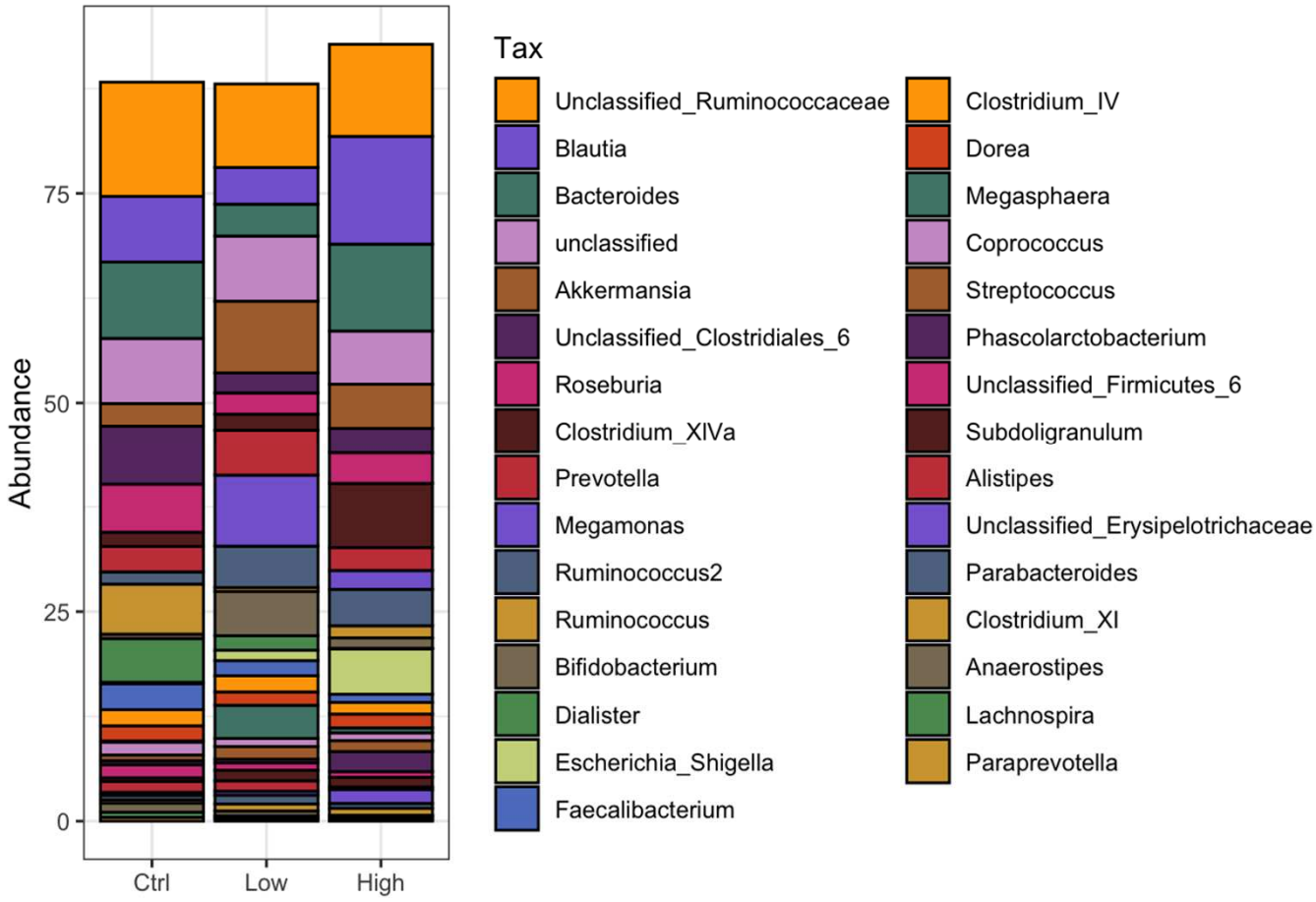

Supplementary Fig.7 Relative abundance of the different genera in AUD patients with high and low intestinal permeability (IP) and controls.

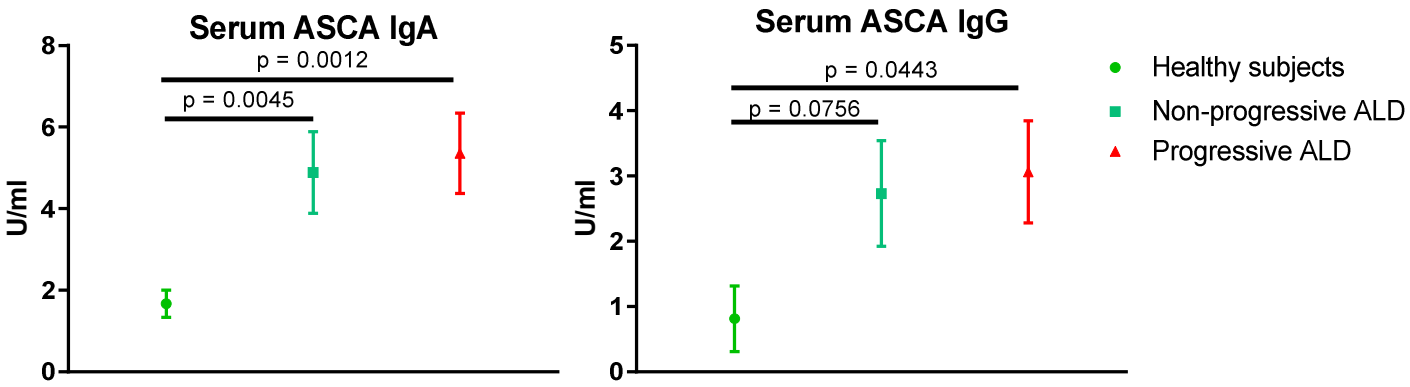

Supplementary Fig.8 Changes of serum ASCA levels in AUD patients in association with severity of liver disease.

Serum ASCA IgA and IgG increased independently from liver disease severity and were already significantly upregulated in non-progressive ALD compared to controls.

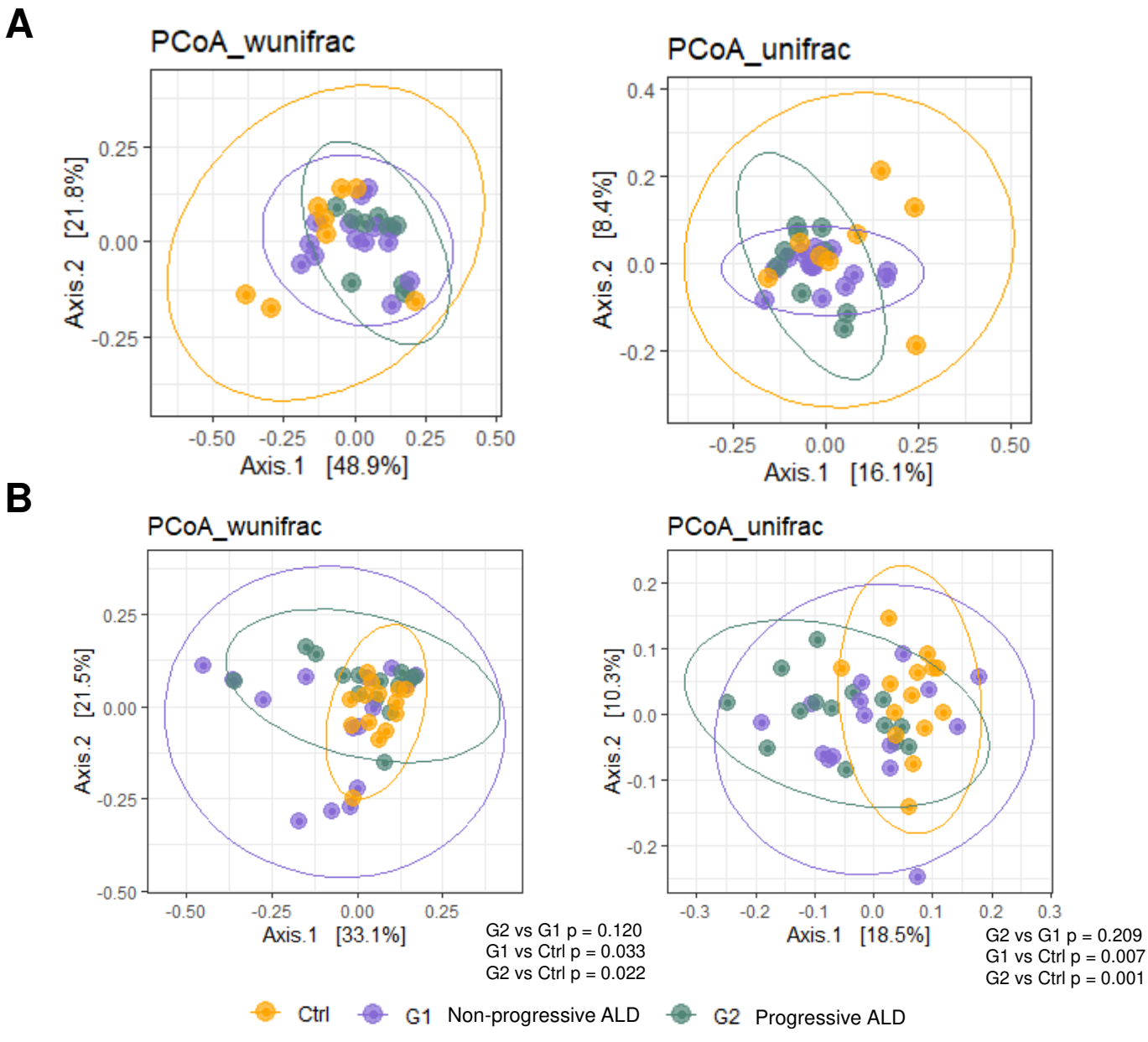

Supplementary Fig.9 Microflora composition in both duodenum and stools according to stage of liver disease.

Microbial composition (β diversity) of the duodenal mucosa-associated **(A)** and fecal (**B**) microbiota did not change in relation to ALD severity in AUD patients.

A

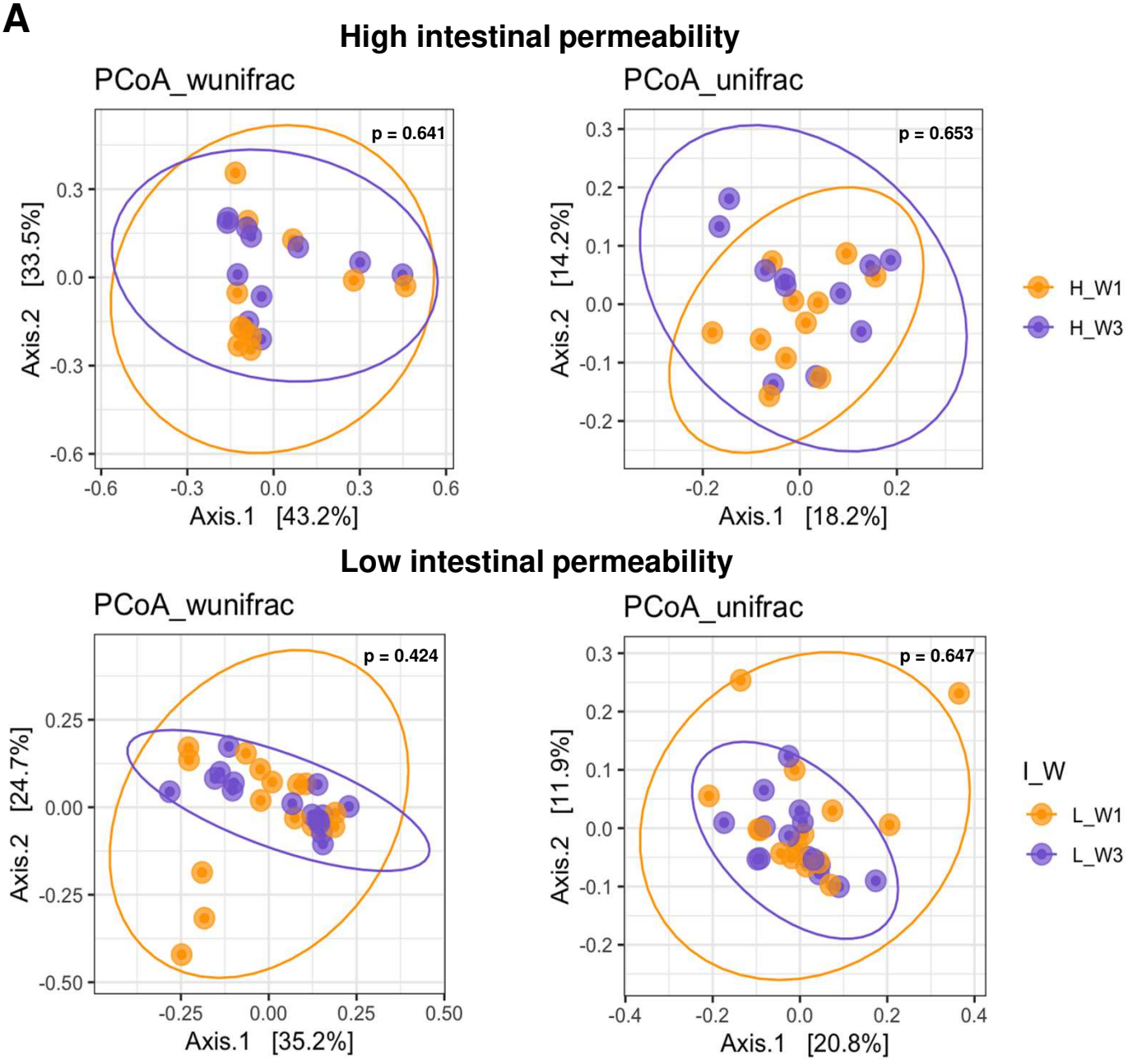
High intestinal permeability
PCoA_wunifrac
p = 0.641
Axis.2 [33.5%]
Axis.1 [43.2%]
PCoA_unifrac
p = 0.653
Axis.2 [14.2%]
Axis.1 [18.2%]
H_W1
H_W3
Low intestinal permeability
PCoA_wunifrac
p = 0.424
Axis.2 [24.7%]
Axis.1 [35.2%]
PCoA_unifrac
p = 0.647
Axis.2 [11.9%]
Axis.1 [20.8%]
I_W
L_W1
L_W3

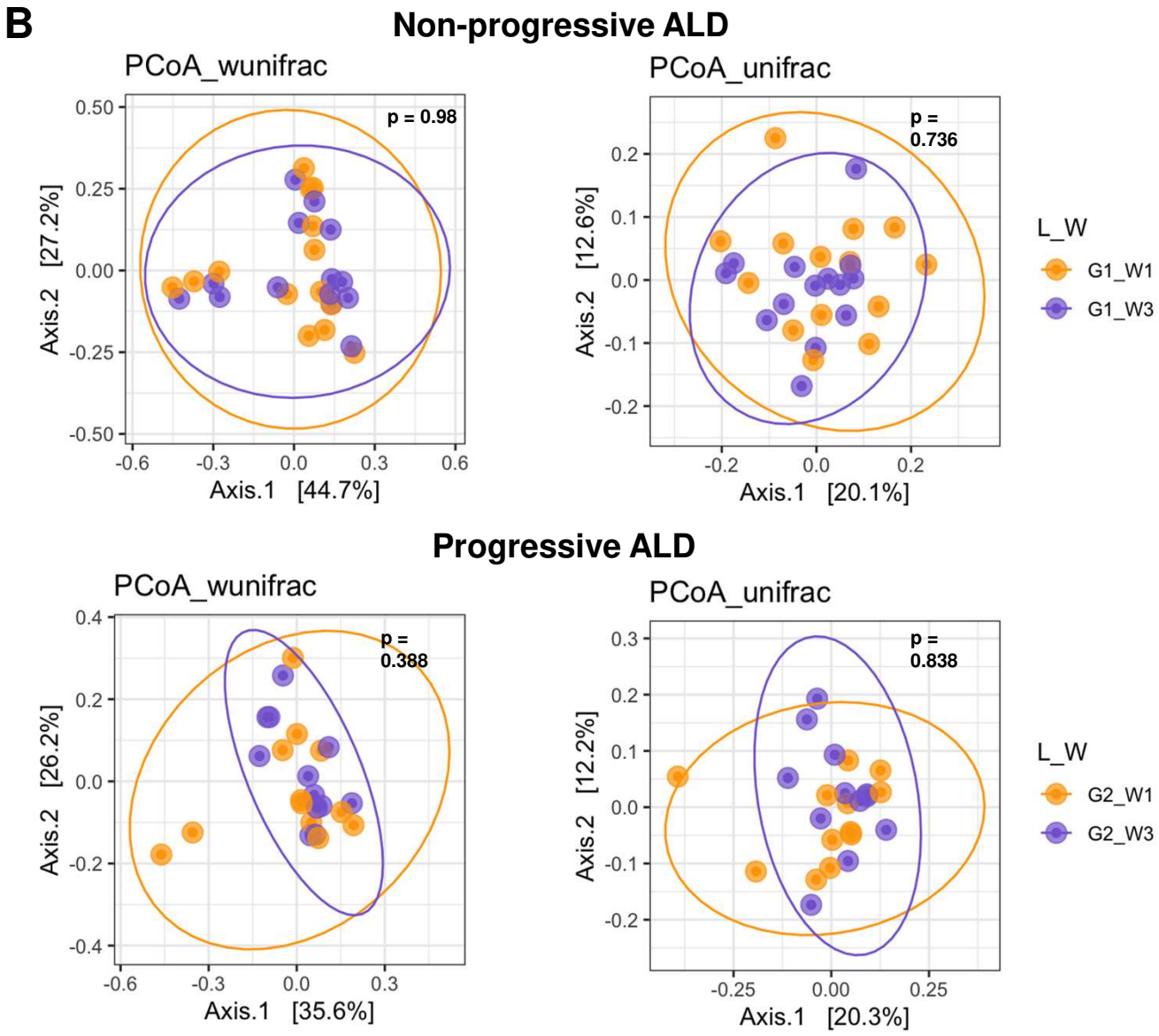

Supplementary Fig.10 Microbial profiles in the stools of AUD patients after abstinence. Microbial composition (β diversity) of the fecal microbiota did not change after abstinence in AUD patients subdivided according to both intestinal permeability (**A**) and ALD stage (**B**).

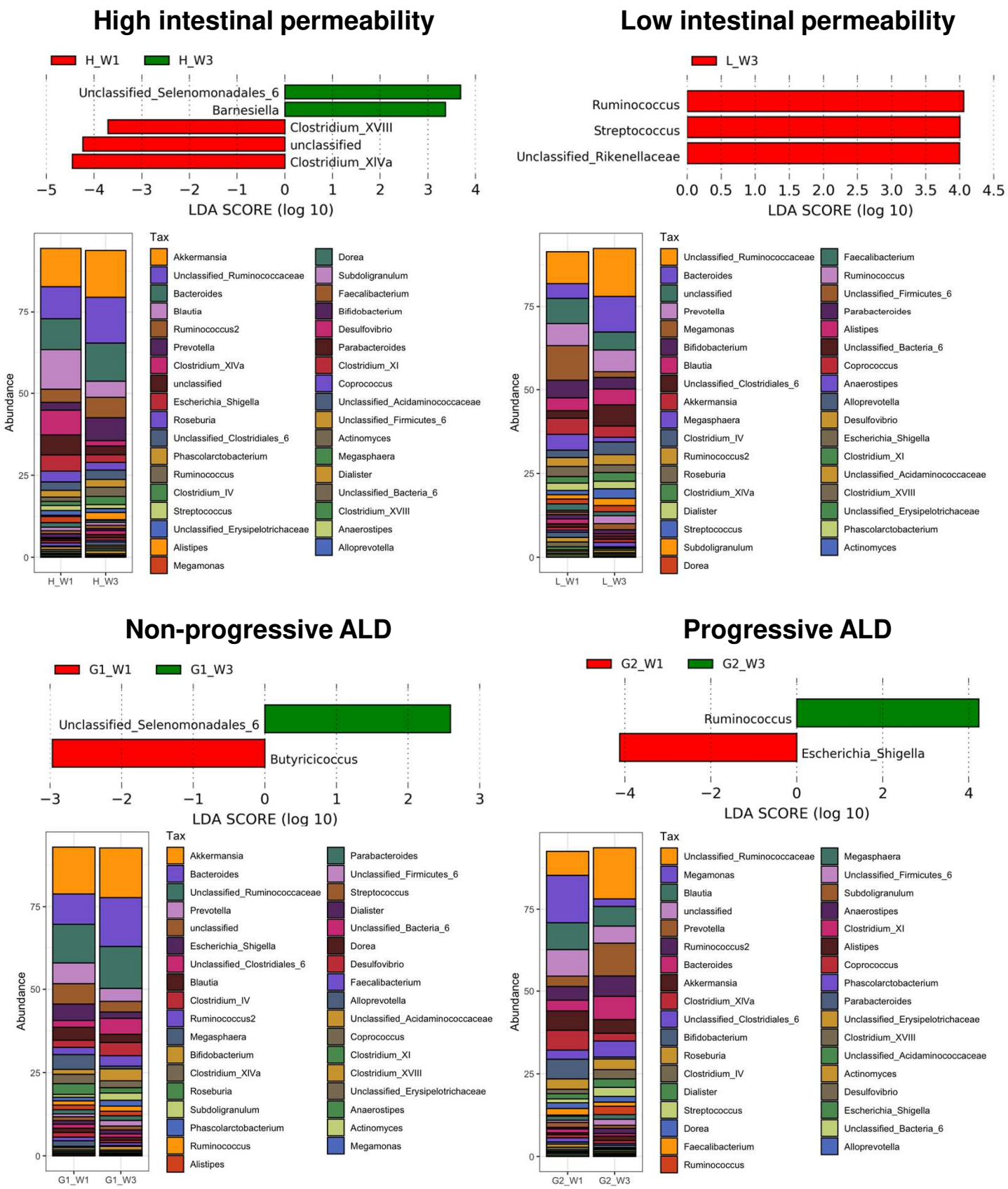

Supplementary Fig.11 Linear discriminating analysis (LDA) and relative abundance of bacterial genera in the stool of AUD patients, subdivided according to both intestinal permeability and ALD stage, after abstinence.